10.1 Materials

Lenalidomide (LND) was obtained as a gift sample from Apicore Pharmaceutical Ltd, Vadodara (India). Cell culture plates (96, 12 and 6 well plates), culture flasks, Dulbecco's Modified Eagle Medium (DMEM), Hank's Balanced Salt solution (HBSS), fetal bovine serum (FBS), Trypsin-EDTA, penicillin-streptomycin solution (100 U/ml), fluorescein isothiocyanate (FITC), 1-(4,5-dimethylthiazol-2-yl)-3,5-diphenyl-formazan (MTT) were purchased from Himedia (India). Transwell inserts were purchased from Corning, NY, (USA). Micropipettes were purchased from Thermo fishier Scientifics. Micro tips were purchased from Tarson (India). All other chemicals and solvents used were of analytical grade. The U-373 MG, U-87 MG and MDCK II cell lines were purchased from National Center for Cell Science (NCCS) Pune (India).

Please refer section 9.1 for sources of materials used for the preparation and surface modification of LNPs and Lf-LNPs

10.2 Equipments

- Digital analytical balance (ATX224 Shimadzu, Japan)
- Cooling centrifuge (Remi equipment Pvt Ltd, India)
- Magnetic stirrer (Remi sci. Equipment, India)
- Deep freezer (EIE Inst. Ltd, Ahmedabad)
- Sonicator: Modern Industrial Corporation (Mumbai, India)
- Fluorescence Microscope: FSX100 (Olympus, USA
- Flow Cytometer: BD FACS Aria III (BD Biosciences, CA)
- BD FACS Diva software version 6.1.3
- Fluorescence Microplate Reader: Fluoroskan Ascent CF (Labsystems, USA)
- Confocal Microscope: Zeiss LSM 510 confocal microscope (Germany)
- ELISA Plate reader: Bio-Rad, Hercules, CA, USA

10.3 Methods

10.3.1 Cell culture protocols

Please refer section 7.3.1 for cell culture protocols.

10.3.2 *In vitro* BBB Passage Study

The permeation of LND, LNPs and Lf-LNPs across the BBB was assessed by *in vitro* BBB model (co-culture model) (1). After development of co-culture model (refer section 7.3.2), 1 ml of LND, PNPs, LNPs, Lf-PNPs and Lf-LNPs at LND concentration of 2 mg/ml was added to the luminal compartment of inserts. Then, 200 µl of medium was withdrawn from the basal compartment at predetermined time interval (0, 2, 24 and 48 h), replacing with fresh medium. The permeation of drug through the *in vitro* BBB model was determined by spectrofluorophotometer (refer section 3.8) (1) and transport ratio of LND, LNPs and Lf-LNPs was determined using the following equation:

$$Transportatio\ (\%) = \left(\frac{Wn}{W}\right) * 100 \quad \text{.....Equation 10.1}$$

Where, Wn = amount of LND in the basal chamber at time "n" (n = 2, 24 and 48 h); W = amount of LND added in the apical chamber.

10.3.3 *In-vitro* cell viability assay

The *in-vitro* cell cytotoxicity of the prepared nanoparticles (LNPs and Lf-LNPs along with pure LND) against U-87 MG cells was estimated by MTT assay as procedure mentioned in section 7.3.3. Cells were incubated with different concentrations (10-50 µg/ml) of pure LND, PNPs, LNPs, Lf-PNPs and Lf-LNPs for 24 and 48 h, respectively and cytotoxicity was determined using MTT reagent (2).

10.3.4 Cellular uptake and uptake mechanism

The uptake poisoning method was utilized to investigate the cellular uptake and endocytosis mechanism of LND, PNPs, LNPs, Lf-LNPs and FITC conjugated Lf-PNPs in U-87 MG cell monolayers. U-87 MG cells (1×10^5 cells/well) were seeded on 6-well plate and allowed to grow for 24 h. After 24h, old media was replaced with fresh culture medium containing sodium azide (0.1 % w/v), chlorpromazine (10 µg/ml) and nystatin (50 µg/ml) and cell monolayers were incubated for 1 h at 37 °C. After 1 h, LND, LNPs, Lf-LNPs and FITC Lf-PNPs (25 µg/ml each) were added and co-incubated for 4 h. After incubation, cells were lysed using 1% Triton X-100

and amount of LND and FITC inside the cells was analyzed by measuring fluorescence using spectrofluorophotometer (2,3).

10.3.5 Lactoferrin (Lf) receptor targeting assay

Lf receptor blocking assay was used to study uptake of Lf-LNPs by Lf receptor. For that, the cells were pretreated with Lf (100 µg/ml) for 30 min followed by washing and treatment with FITC conjugated Lf-LNPs, again incubated for an additional 4h. After incubation, cells were lysed using 1% Triton X-100 and amount of FITC inside the cells was analyzed by spectrofluorophotometer (3) .

10.3.6 Reactive oxygen species (ROS) generation study

Dichlorofluorescein (DCF) assay was utilized to estimate ROS generation in U-87 MG cells. The cells were seeded in 96 well plate and incubated for 24 h. After 24h, medium was replaced with fresh medium containing LND, PNPs, LNPs, Lf-PNPs and Lf-LNPs (10-50 µg/ml). In this analysis, 10 µg ml^{-1} of H_2O_2 was used as a positive control while untreated cells were used as negative control. Cells were harvested, washed once with PBS and incubated with 10 µM H_2DCFDA (2,7-dichlorodihydrofluorescein diacetate) (in PBS 1×) for 30 min at 37°C prior to analysis. The DCF fluorescence was then recorded at 535 nm using a plate reader (Fluoroskan Ascent CF (Labsystems, USA)). The generated ROS was expressed as a ratio of the fluorescence of DCF of treated cells to that of untreated cells (2).

10.3.7 Scratch assay

U-87 MG cells (2×10^5 cells/ well) were plated in 6-well plates and incubated at 37°C and 5% CO_2 environment to form a confluent monolayer. After monolayer formation, scratch was created with the help of p200 pipette tip. The scratch containing cells were washed with growth medium to remove the debris and smoothening of scratch. Then old media was replaced with 1 ml of fresh medium specific for the in vitro scratch assay. To obtain the same field during the image acquisition, markings were created to be used as reference points close to the scratch. Then cells were treated with LND, LNPs and Lf-LNPs at a concentration equivalent to 25 µg/ml of LND. In control group wells, no sample was added. Then plates were incubated at 37 °C and examined daily until the scratch in the control group wells was filled completely with cells (4)

10.4 Results and discussion

10.4.1 *In vitro* BBB passage/ flux study

The passage of the developed nanoparticles through BBB was assessed by constructing *in vitro* co-culture BBB model using U-373MG cells (as glial cells) and MDCK cells (as endothelial cells). *In vitro* BBB passage of pure LND, PNPs, LNPs, Lf-PNPs and LF-LNPs were estimated and results are summarized in Figure 10.1. The results indicated that the transport efficiency of pure LND, PNPs, LNPs, Lf-PNPs and LF-LNPs increased in a time dependent manner. The transport ratio of Lf-PNPs and Lf-LNPs was more than pure LND, PNPs and LNPs through the BBB model at all the tested time points: LND < PNPs < LNPs < Lf-PNPs < Lf-LNPs which may be due to Lf surface modification and indicated higher BBB passage ability of Lf-PNPs and Lf-LNPs as compared to pure LND, PNPs and LNPs. The higher BBB passage ability of Lf-PNPs and LF-LNPs may be due to lactoferrin receptor mediated uptake as lactoferrin receptors are over expressed in the BBB which facilitate the passage of lactoferrin modified nanoparticles (3) As compared to LND and LNPs, LF-LNPs demonstrated 1.86 folds and 1.12 folds higher transport across BBB respectively.

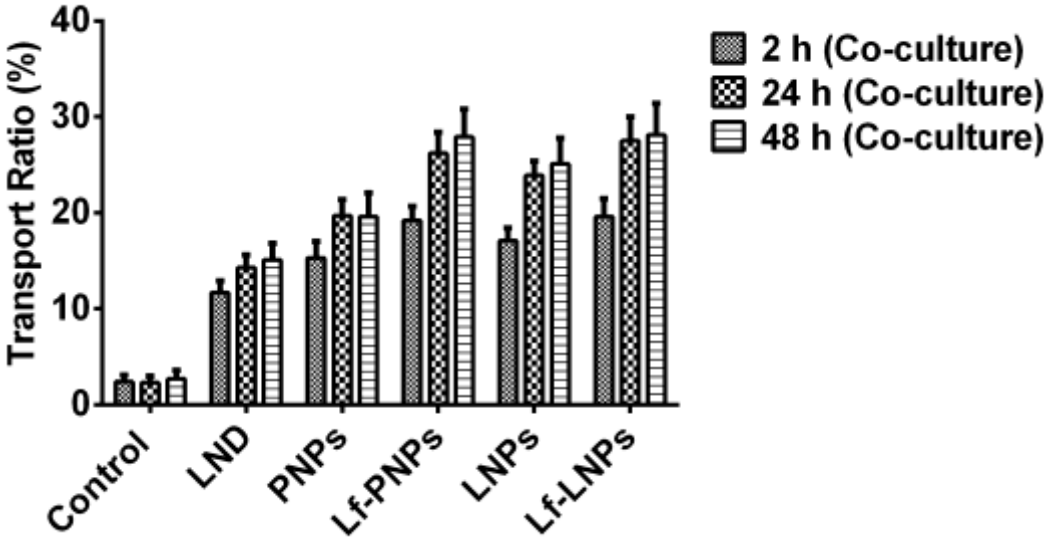

Figure 10.1: *In vitro* BBB passage studies for pure LND, PNPs, LNPs, Lf-PNPs and Lf-LNPs after 2h, 24h and 48h

10.4.2 In vitro cell viability assay

MTT assay was performed to assess cell viability of LND, PNPs, LNPs, Lf-PNPs and Lf-LNPs and results indicated concentration dependent suppression of cell viability. As compared to LND and LNPs, Lf-LNPs demonstrated 50 % suppression of cell viability (figure 10.2). Lf-LNPs demonstrated 50.1 % ± 3.6 % cell viability at 50 µg/ml concentration after 48 h while pure LND and LNPs showed 75.4 % ± 3.8 % and 57.2 ± 2.9 % cell viability respectively. As compared to LND and LNPs, Lf-LNPs showed 1.50 folds and 1.14 folds higher suppression of cell viability respectively. The reason of higher suppression of cell viability in case of Lf-LNPs may be due to slow release and longer retention of LND from Lf-LNPs as compare to pure LND and LNPs hence cytotoxicity of Lf-LNPs was more (5). Apart from this, uptake of Lf-LNPs was more as compared to LND and LNPs due to surface modification with Lf which facilitated the Lf receptor mediated uptake of Lf-LNPs (Lf receptor also over expressed in brain tumor cells) and led to suppression of cell viability (3). In case of PNPs and Lf-PNPs, suppression of cell viability was 97.4 % ± 3.2 % and 98.1 % ± 2.9 % respectively which demonstrated that placebo nanoparticles were non toxic and biocompatible.

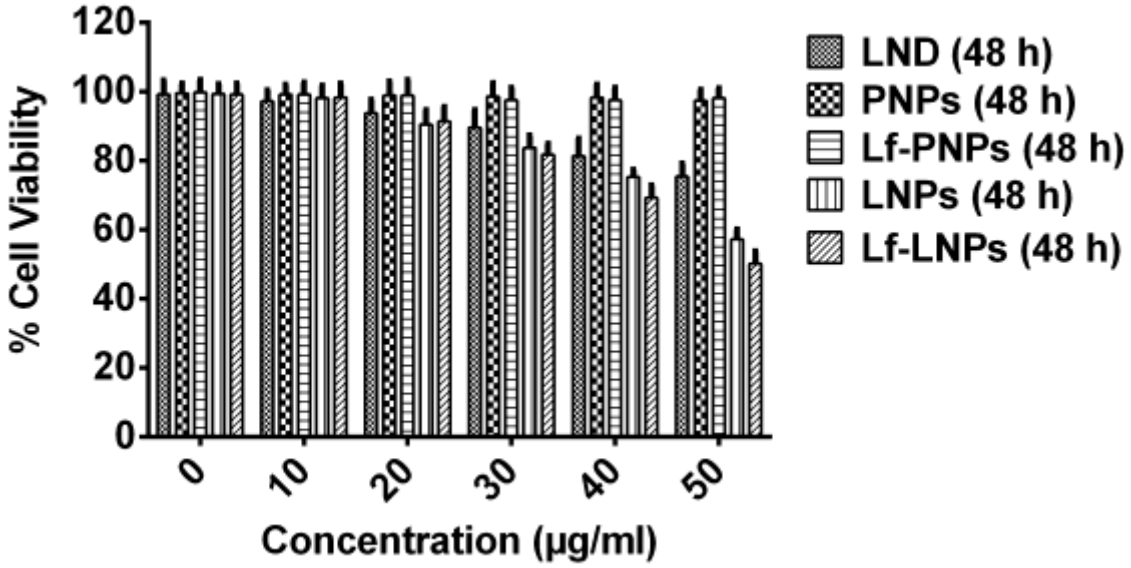

Figure 10.2: *In vitro* cell viability study in U-87MG cells after 48 h. Data is represented as mean ± SD (n = 3)

10.4.3 Cellular uptake

Quantitative cellular uptake of LND, LNPs, Lf-PNPs and Lf-LNPs on U-87 MG cells were assessed and results are shown in figure 10.3. As compared to LND, higher uptake of LNPs was observed which may be due to albumin. As mentioned earlier, albumin binding receptors (SPARC and gp-60) are over expressed in U87 MG cells for transportation of albumin (8) so LNPs might be bind to these receptors which enhanced the uptake of LNPs. Apart from this, albumin also triggers the endocytosis into tumors cells which was further confirmed by demonstration of cellular uptake mechanism. In case of Lf-PNPs and Lf-LNPs, uptake of Lf-PNPs and Lf-LNPs were more as compared to LND and LNPs which may be due to presence of Lf over the surface of PNPs and LNPs. Surface modification of LNPs with Lf may have facilitated Lf receptor mediated uptake of Lf-LNPs and led to higher uptake than LNPs (3). This was further confirmed by demonstration of cellular uptake mechanism.

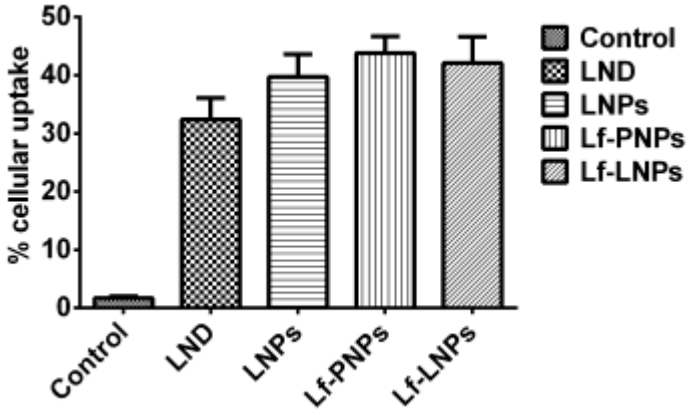

Figure 10.3: Cellular uptake of LND, LNPs, Lf-PNPs and Lf-LNPs in U87 MG cells. Data is represented as mean ± SD.

10.4.4 Cellular uptake mechanism

Various receptor poisons were used to study the uptake mechanism in which chlorpromazine, nystatin and sodium azide were used to inhibit clathrin, caveolae and cell energy metabolism respectively (3). Cellular uptake mechanism of LND, LNPs, Lf-PNPs and Lf-LNPs across U-87 MG cell monolayer was evaluated (figure 10.4). The results demonstrated that cellular uptake of LND in presence of chlorpromazine was significantly reduced to 8.3 % ± 0.7% after 4 h while in

presence of nystatin and sodium azide, reduction in uptake was 20.4% ± 1.7% and 12.0 % ± 1.1 % after 4 h respectively. From the results, it can be concluded that caveolae mediated endocytosis may be involved in the uptake of LND across the U87MG cell monolayer. In case of LNPs, reduction in cellular uptake after 4 h was found to be 18.4 % ± 1.4 % (in presence of chlorpromazine), 21.4 % ± 1.1 % (in presence of nystatin) and 20.4 % ± 1.9 % (in presence of sodium azide) respectively. From the results, it can be concluded that caveolae mediated endocytosis may be involved in the uptake of LNPs across the U-87MG cell monolayer. The obtained results were also accordance with reported literature (7). In case of Lf-PNPs and Lf-LNPs, reduction in cellular uptake after 4 h incubation was found to be 30.4 % ± 2.4 % and 31.8 % ± 2.3 % respectively (in presence of chlorpromazine), 27.4 % ± 1.9 % and 29.7 % ± 1.2 % respectively (in presence of nystatin) and 23.7 % ± 1.7 % and 22.1 % ± 1.2 % respectively (in presence of sodium azide). From the results, it can be concluded that reduction in uptake was maximum when chlorpromazine (clathrin pathway inhibitor) was used; so clathrin mediated endocytosis may also be involved in the uptake of Lf-PNPs and Lf-LNPs across the U-87 MG cell monolayer. The obtained results were also accordance with previously reported literature (8)

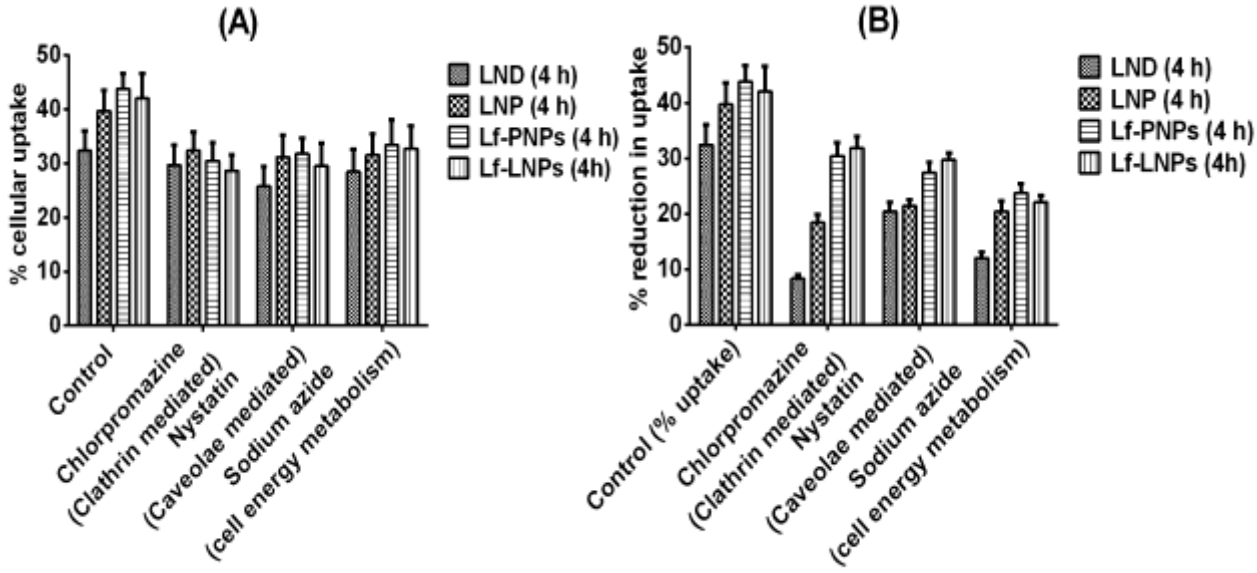

Figure 10.4: Elucidation of cellular uptake mechanism of LND, LNPs, LF-PNPs and Lf-LNPs (A) percent cellular uptake and (B) reduction in cellular uptake. Data is represented as mean ± SD (n = 3)

10.4.5 Lactoferrin receptor targeting assay

To verify the Lf receptor mediated uptake of Lf-LNPs, Lf receptor blocking assay using excess amount of Lf (100 μg/ml) as Lf receptor inhibitor was used. The results of Lf blocking assay indicated significant reduction in cellular uptake of Lf-LNPs in Lf treated U-87 MG cells as before Lf receptor blocking; uptake was higher (figure 10.5). Free Lf (as an inhibitor) hindered the binding of Lf-LNPs with the receptor. The reduction in cellular uptake of Lf-LNPs after 4 h was found to be 56.1 % ± 2.4 %. These results confirmed Lf mediated uptake of Lf-LNPs. In case of LNPs no significant reduction in uptake was observed which confirms that uptake of LNPs was not Lf mediated. From all the obtained results, we can conclude that cellular uptake and internalization of Lf-LNPs was predominantly via endocytosis and Lf receptor mediated uptake.

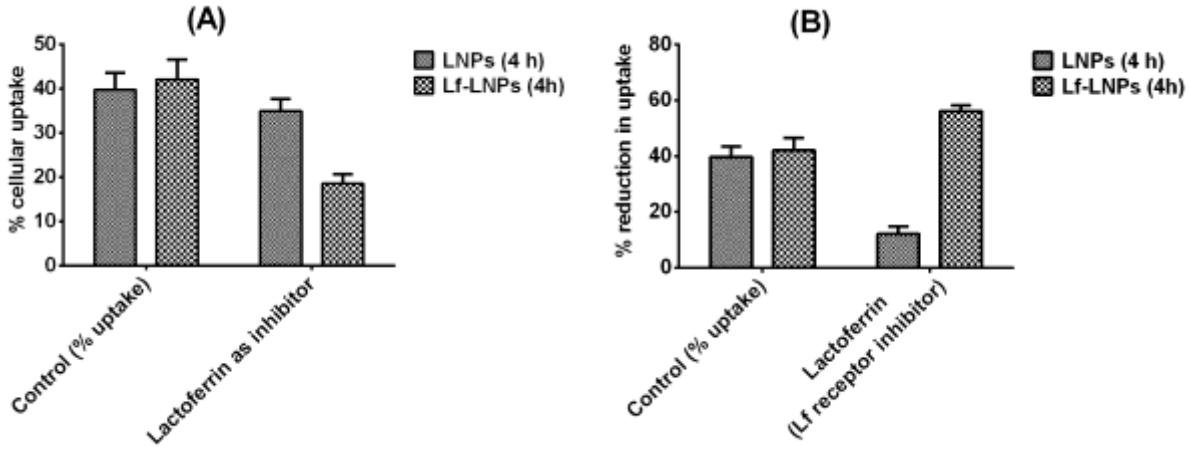

Figure 10.5: Lactoferrin receptor binding assay of LNPs and Lf-LNPs (A) % uptake and (B) % reduction in uptake

10.4.6 ROS generation study

The ROS generation potential of LND, PNPs, Lf-PNPs, LNPs and Lf-LNPs were assessed in U-87 MG cells by DCF assay (9). The results as shown in figure 10.6 demonstrated concentration dependent ROS generation of LND, LNPs and Lf-LNPs. The untreated cells (negative control), PNPs and Lf-PNPs did not show any ROS generation while LNPs and Lf-LNPs demonstrated higher ROS generation as compared LND but lesser ROS generation than positive control

(H_2O_2). The LNPs and Lf-LNPs indicated 1.13 folds and 1.43 folds increase in ROS generation respectively as compared to pure LND. The obtained results may be correlated with the fact that increase in concentration of LNPs and Lf-LNPs led to increased concentration of released LND leading to increase in ROS generation. Lf-LNPs showed higher ROS generation as compared to pure LND and LNPs. This may be due to higher uptake of Lf-LNPs via Lf receptor which led to increased LND concentration in the cells that ultimately caused increased ROS generation that led to oxidative stress to the cells, inhibited the cell proliferation and caused cell death (7).

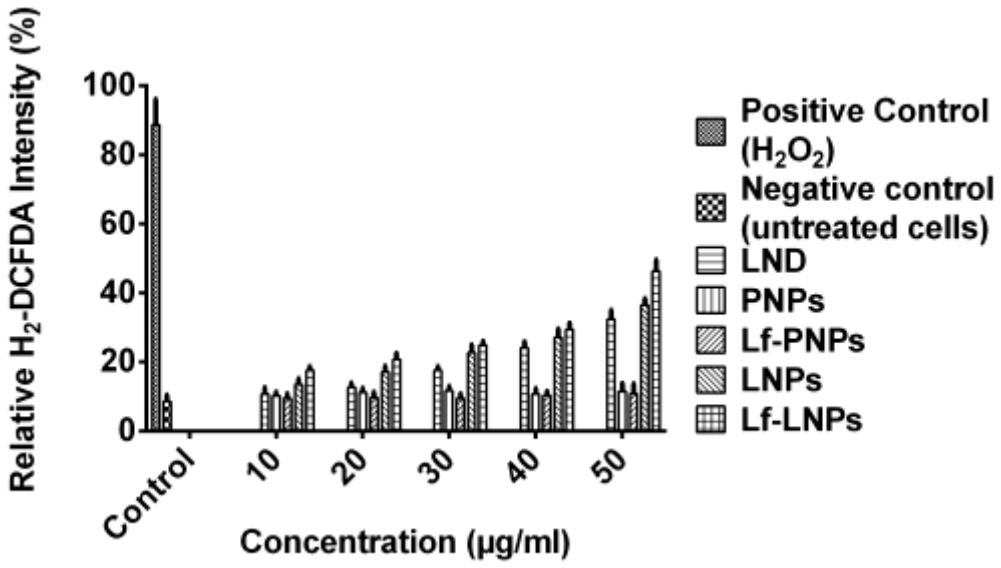

Figure 10.6: Quantitative determination of ROS generation of LND, PNPs, LF-PNPs, LNPs and Lf-LNPs. Data represented as mean ± SD

10.4.7 Scratch assay

The results of scratch assay are demonstrated in figure 10.7. The results indicated slower cell migration as compared to control group after treatment with LND and developed nanoparticles. As compared to LND and LNPs, Lf-LNPs indicated significant restriction of cell migration.

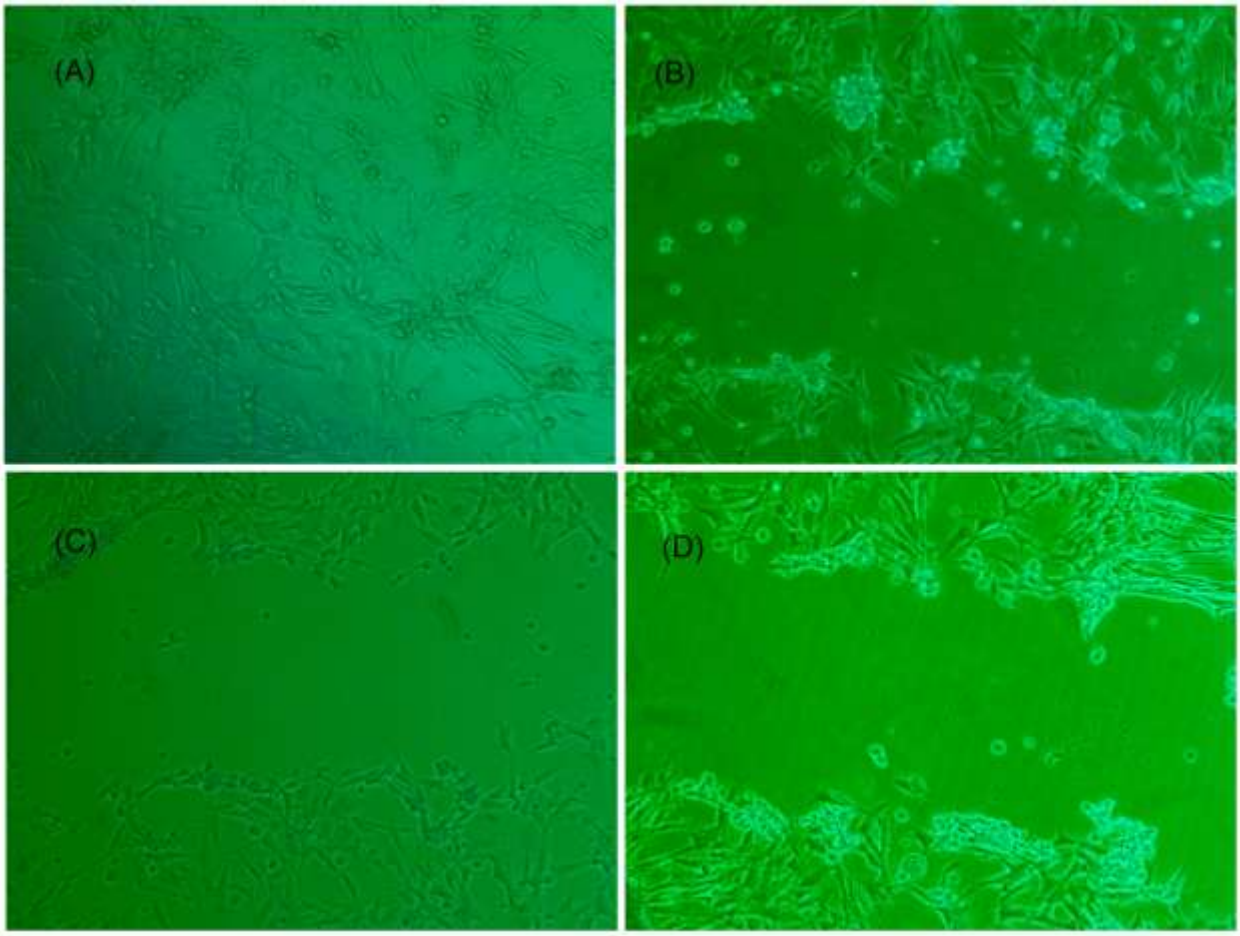

Figure 10.7: *In vitro* scratch assay to determine effect of different formulations on cell migration: (A) Control, (B) LND, (C) LNPs and (D) Lf-LNPs

References

1. Jain D, Bajaj A, Athawale R, Shrikhande S, Goel PN, Nikam Y, et al. Surface-coated PLA nanoparticles loaded with temozolomide for improved brain deposition and potential treatment of gliomas: development, characterization and in vivo studies. Drug Deliv. 2016;23(3):999–1016.

2. Pandey A, Singh K, Patel S, Singh R, Patel K, Sawant K. Hyaluronic acid tethered pH-responsive alloy-drug nanoconjugates for multimodal therapy of glioblastoma: An intranasal route approach. Mater Sci Eng C Mater Biol Appl. 2019 May;98:419–36.

3. Su Z, Xing L, Chen Y, Xu Y, Yang F, Zhang C, et al. Lactoferrin-modified poly(ethylene glycol)-grafted BSA nanoparticles as a dual-targeting carrier for treating brain gliomas. Mol Pharm. 2014 Jun 2;11(6):1823–34.

4. Liang C-C, Park AY, Guan J-L. In vitro scratch assay: a convenient and inexpensive method for analysis of cell migration in vitro. Nature Protocols. 2007 Feb;2(2):329–33.

5. Pulakkat S, Balaji SA, Rangarajan A, Raichur AM. Surface Engineered Protein Nanoparticles With Hyaluronic Acid Based Multilayers For Targeted Delivery Of Anticancer Agents. ACS Appl Mater Interfaces. 2016 Sep 14;8(36):23437–49.

6. Lin T, Zhao P, Jiang Y, Tang Y, Jin H, Pan Z, et al. Blood–Brain-Barrier-Penetrating Albumin Nanoparticles for Biomimetic Drug Delivery via Albumin-Binding Protein Pathways for Antiglioma Therapy. ACS Nano. 2016 Nov 22;10(11):9999–10012.

7. Kudarha RR, Sawant KK. Chondroitin sulfate conjugation facilitates tumor cell internalization of albumin nanoparticles for brain-targeted delivery of temozolomide via CD44 receptor-mediated targeting. Drug Deliv and Transl Res [Internet]. 2020 Oct 7 [cited 2020 Oct 24]; Available from: https://doi.org/10.1007/s13346-020-00861-x

8. Chen Z, Chen J, Wu L, Li W, chen jun, Cheng H, et al. Hyaluronic acid-coated bovine serum albumin nanoparticles loaded with brucine as selective nanovectors for intra-articular injection. IJN. 2013 Oct;3843.

9. Rakotoarisoa M, Angelov B, Garamus VM, Angelova A. Curcumin- and Fish Oil-Loaded Spongosome and Cubosome Nanoparticles with Neuroprotective Potential against H2O2-Induced Oxidative Stress in Differentiated Human SH-SY5Y Cells. :2.